Optica Applicata, Vol. XLVIII, No. 3, 2018
10.5277/oa180306

Optimal mass transportation problem and freeform optics design – the identity of optimization scheme and the numerical solution method

JACEK WOJTANOWSKI

Institute of Optoelectronics, Military University of Technology,
gen. Sylwestra Kaliskiego 2, 00-908 Warszawa, Poland

*Corresponding author: jacek.wojtanowski@wat.edu.pl

Due to outstanding light shaping potential, freeform optical surfaces have been considered theoretically from centuries. Recently, they gained increased interest due to the availability of manufacturing technologies. Nevertheless, the design of freeform surfaces still becomes a challenge, associated with advanced mathematical concepts and significant computing power. In this work, a very interesting unification of theories is mentioned. It is shown how the problem of optimal redistribution of mass, analyzed in the 18th century, corresponds to the problem of optical beam shaping realized by freeform surface. Both issues are governed by the same partial differential equation. In the paper, a novel numerical algorithm for solving this partial differential equation is discussed. As an example, a design of freeform lens, capable of casting completely arbitrary shapes, is presented.

Keywords: optical design, freeform lens, beam shaping, non-imaging optics.

1. Introduction

French mathematician Gaspard Monge (1746–1818) considered in 1781 the problem of fortification system (fr. *remblais*) construction [1]. These considerations aimed at the cost minimization of such investment (Fig. 1), which technically was modelled as extracting sand (fr. *déblais*) at points $\mathbf{x}$ and transporting it to the target site associated with points $\mathbf{y} = T(\mathbf{x})$. The cost of transport was directly proportional to the distance between $\mathbf{x}$ and $\mathbf{x}'$. This gave rise to an extensive section of mathematics related to the so-called optimal mass transportation (OMT).

For many decades, this theory did not see application potential and remained in the purely abstract area. In the 1940s, Russian mathematician and economist, Leonid Kantorovich (1912–1986), the Nobel Prize winner in Economics, took up and developed the problem in the context of supplying the network of cafes through the network

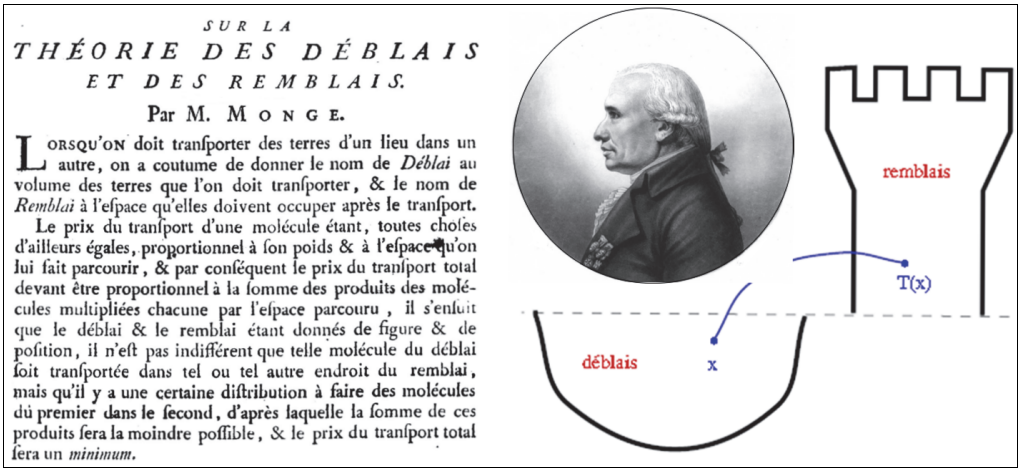

Fig. 1. Optimal mass transportation problem – historical perspective (left – photo of the original paper by MONGE [1], middle – Monge's portrait, right – graphical explanation of OMT).

of bakeries. Nowadays, the usefulness of the mathematical apparatus associated with the theory of optimal transport no longer needs to be persuaded. It finds application in astonishingly many areas of science and technology, including image analysis, economics, forensics, medicine, architecture and many more.

From mathematical perspective, OMT problem can be defined generally as the optimization of the following integral:

$$\begin{cases} \int\limits_X c(\mathbf{x}, T(\mathbf{x}))\, f(\mathbf{x})\,\mathrm{d}\mathbf{x} \\ T\colon\ f(\mathbf{x}) \to g(\mathbf{x}') \end{cases} \tag{1}$$

where $f(\mathbf{x})$ is the initial mass distribution in X space, $g(\mathbf{x}')$ is the final (desired) mass distribution in X' space, $c(\mathbf{x}, \mathbf{x}')$ is the assumed cost function and $T(\mathbf{x})$ is the unknown transformation function. In other words, OMT problem comes down to finding such mass-preserving transformation function T, which minimizes the integral given in Eq. (1). Such generalization of Monge OMT formulation (where the cost function was simply $c(\mathbf{x}, \mathbf{x}') = |\mathbf{x} - \mathbf{x}'|$) is called the Monge–Kantorovich problem [2]. In one-dimensional space (x, x' – scalars), this problem is trivial, however, in two dimensions (and higher), solution methods require the application of advanced concepts and sometimes they do not exist. ROCKAFELLAR proved in [3], that the Monge–Kantorovich problem in 2D space, with the quadratic cost function $c(\mathbf{x}, \mathbf{x}') = 0.5\,|\mathbf{x} - \mathbf{x}'|^2$ is identical with the second order nonlinear partial differential equation (PDE) of the Monge–Ampère type: $\det \nabla^2 \psi(\mathbf{x}) = g(\mathbf{x}, \nabla\psi)$. It was shown that the solution $T(\mathbf{x})$ has to be a gradient of

certain scalar convex function $\psi(\mathbf{x})$, which can be found from the following variant of the a.m. Monge–Ampère PDE:

$$\det \nabla^2 \psi(\mathbf{x}) = \frac{f(\mathbf{x})}{g(\nabla \psi(\mathbf{x}))} \tag{2}$$

Connection between OMT problem and optical intensity shaping was reported in numerous publications. General mathematical treatment of irradiance and wavefront transformation in double-reflector or double-refractor configuration can be found in [4–6]. Authors proved that optical surfaces can be obtained from the minimization of certain action functionals, which essentially coincide with a variational approach to Monge–Kantorovich OMT. These papers however were focused on mathematical aspects of general solution existence and surface properties and did not indicate direct solution methods. On the other side, RIES and MUSCHAWECK in [7] deal with a very specific case of casting three-letters-shape by a single freeform surface, which is similar to the problem discussed in this paper. The authors however, apply a totally different mathematical approach, dealing with wavefront curvature transformation and the corresponding surface curvature tensor, which can be obtained from a set of partial differential equations. Although an exemplary freeform lens design was presented in this paper, no practical computational details were revealed. Several other different numerical methods of freeform optical surfaces were also reported. In [8] FOURNIER *et al*. describe the algorithm based on the determination of the appropriate source-target ray mapping which is obtained from a collection of supporting ellipsoids forming a piece -by-piece freeform mirror. Similar methodology, however oriented for refractive lenses is provided in [9] where the authors synthesize surfaces from Cartesian ovals. Unfortunately, both *supporting-ellipsoids* and *supporting-ovals* methods are limited to relatively low resolution distributions. To overcome such limitations, BRUNETON *et al*. proposed least-squares optimization procedure [10], however devoted to multiple freeform surface configurations. Another method to calculate freeform lens able to cast high-resolution irradiance patterns was reported in [11]. Authors first find integrable ray mapping by solving a linear advection equation and then build optical surface by solving standard integrals. This method does not apply elliptic Monge–Ampère PDE, however its performance is also remarkable. Unfortunately, calculation details are not forwarded precisely, which makes it difficult to reproduce them for individual needs. It should be clearly stated that OMT problem is not only associated with elliptic Monge–Ampère PDE. For example in [12, 13] in order to control both irradiance and wavefront, the authors design double freeform surfaces configurations by the application of the adaptive mesh method based on parabolic Monge–Ampère PDE in the first case and ray-mapping PDE in the second case.

In recent years, the authors of several publications dealt directly with numerical methods of freeform optical design, based on the elliptic Monge–Ampère PDE as it

appears in Eq. (2). In [14] WU *et al*. report successful fabrication of single-freeform -surface lens by the application of a slow tool servo machine. It was shortly mentioned that the surface was calculated by numerically solving elliptic Monge–Ampère PDE, using standard finite-difference discretization. In [15] the same research group provided more computational details of the algorithm, which is based on Newton optimization scheme. Completely different discretization of Monge–Ampère PDE based on Hessian diagonal engineering was proposed in [16]. This approach is devoted however for freeform reflector design. In [17] BRIX *et al*. deal with Monge–Ampère PDE by the application of the so-called collocation method, which again eventually ends up in Newton-type optimization scheme.

In this paper, the alternative numerical methodology of solving Eq. (2) is given in details. Instead of popular Newton scheme, the Gauss–Seidel iteration approach is proposed. It allows one to obtain the solution of elliptic Monge–Ampère PDE without any accurate idea of initial guess. On the other hand, Newton method in this context requires a good candidate to start iterations with. If such initial guess cannot be well invented, the solution may not converge to global minimum and stuck in local one, providing unsatisfactory solution. As such, in popular algorithms reported so far, initial guess assessment sometimes creates more difficult problem than the solution of Monge–Ampère PDE itself. Essentially it was the motivation for the presented research.

The paper is organized as follows. In Section 2, step-by-step derivation of Monge –Ampère PDE governing refraction of a collimated beam on a single freeform surface is provided in a simplified way. Direct correspondences between mechanical quantities from OMT theory and optical quantities are indicated. In Section 3, the novel numerical procedure of solving elliptic Monge–Ampère PDE is given in details. Challenging exemplary design of a freeform lens is discussed in Section 4, where the proposed algorithm is used and its performance is verified. Paper is summarized with short conclusions and references.

2. Mathematical model of irradiance transformation resulting from refraction on freeform surface

The issue of OMT seems to be applicable also in the context of an unconventional freeform optics design. This type of refractive (lenses) or reflective (mirrors) components do not show any symmetry [18]. Because of freeform surfaces manufacturing capabilities [19], which have become available in recent years, this type of optics is becoming the only choice in a number of novel applications and reasonable replacement for classical or diffractive optics [20–22] in variety of existing solutions. Being unconstrained by translational, rotational or any type of symmetry, freeform technology significantly expands the possibilities of light distribution shaping. For example, transforming a Gaussian beam into a triangle, square, or even irregularly shaped beam becomes possible. Seemingly trivial formulation of the OMT problem leads to the discussed nonlinear elliptic Monge–Ampère PDE. The same type of PDE can be easily obtained by the analysis of optical beam refraction on single freeform surface, which

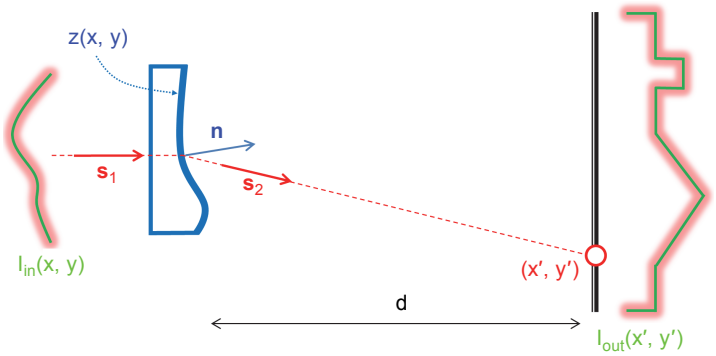

Fig. 2. The geometry of the discussed model – rays of collimated incoming beam go through freeform lens (with entrance surface flat and freeform exit surface), then propagate to the target surface.

for the specific case of collimated input beam refraction on a single freeform surface is shown below.

Let's consider a collimated beam of light impinging onto the optical refracting surface (Fig. 2), described by C_1-class function $z(x, y)$. The input beam can be approached as the collection of rays distributed according to beam power density distribution $I_{\text{in}}(x, y)$. Due to the refraction on the curved surface $z(x, y)$, directions of the rays will change. The aim of this discussion is to find mathematical model describing the power density distribution $I_{\text{out}}(x', y')$ on a flat target located at the distance d. Surface sag function $z(x, y)$ clearly determines normal to this surface vector $\mathbf{n}(x, y)$ distribution, namely:

$$\mathbf{n} = \begin{bmatrix} z_x \\ z_y \\ -1 \end{bmatrix} \tag{3a}$$

$$\hat{\mathbf{n}} = \begin{bmatrix} z_x \\ z_y \\ -1 \end{bmatrix} \frac{1}{\sqrt{z_x^2 + z_y^2 + 1}} \tag{3b}$$

Additionally, without losing generality, let's assume that the incoming beam propagates along z-axis, so one can consider a specific form of $\mathbf{s}_1 = (0, 0, 1)^{\text{T}}$.

Now, in order to find where refracted ray $\mathbf{s}_2$ goes, one can use the Snell law in 3D vector form:

$$\hat{\mathbf{s}}_2 = n_{\text{o}} \hat{\mathbf{s}}_1 - \left\{ n_{\text{o}} (\hat{\mathbf{s}}_1 \cdot \hat{\mathbf{n}}) + \sqrt{1 - n_{\text{o}}^2 \left[1 - (\hat{\mathbf{s}}_1 \cdot \hat{\mathbf{n}})^2 \right]} \right\} \hat{\mathbf{n}} \tag{4}$$

where n_{o} corresponds to the refractive index of the lens glass. Applying the introduced forms of $\mathbf{s}_1$ and $\hat{\mathbf{n}}$ in Eq. (4) leads, after several elementary algebraic transformations, to the following explicit form:

$$\hat{\mathbf{s}}_2 = \begin{bmatrix} \dfrac{n_\mathrm{o} - \sqrt{n_\mathrm{o}^2 + (1 - n_\mathrm{o}^2)(z_x^2 + z_y^2 + 1)}}{z_x^2 + z_y^2 + 1} z_x \\ \dfrac{n_\mathrm{o} - \sqrt{n_\mathrm{o}^2 + (1 - n_\mathrm{o}^2)(z_x^2 + z_y^2 + 1)}}{z_x^2 + z_y^2 + 1} z_y \\ n_\mathrm{o} + \dfrac{\sqrt{n_\mathrm{o}^2 + (1 - n_\mathrm{o}^2)(z_x^2 + z_y^2 + 1)} - n_\mathrm{o}}{z_x^2 + z_y^2 + 1} \end{bmatrix} \tag{5}$$

Having the output vector field $\mathbf{s}_2 = (\mathbf{s}_2^{(1)}, \mathbf{s}_2^{(2)}, \mathbf{s}_2^{(3)})^\mathrm{T}$ determined, it is possible to calculate rays distribution on the target plane located at the distance d, namely:

$$x' = \frac{\mathbf{s}_2^{(1)}}{\mathbf{s}_2^{(3)}} d, \qquad y' = \frac{\mathbf{s}_2^{(2)}}{\mathbf{s}_2^{(3)}} d \tag{6}$$

It should be noted that the above formula is valid for far-field approximation, thus assuming that the lens size is negligible comparing to output distribution. Far field approximation is valid here, because the exact ray positions on the lens are not taken into account. All the rays are treated like going out from its centre which in large distance from the lens does not matter. Taking into account the $\mathbf{s}_2^{(1)}$, $\mathbf{s}_2^{(2)}$, $\mathbf{s}_2^{(3)}$ components, as they are provided in Eq. (5), one obtains:

$$x' = \frac{z_x K(z_x, z_y)}{1 - K(z_x, z_y)} d, \qquad y' = \frac{z_y K(z_x, z_y)}{1 - K(z_x, z_y)} d \tag{7}$$

where

$$K(z_x, z_y) = \frac{n_\mathrm{o} - \sqrt{1 + (z_x^2 + z_y^2)(1 - n_\mathrm{o}^2)}}{z_x^2 + z_y^2 + 1} \tag{8}$$

was introduced for brevity. The functions $x' = f_1(x, y)$, $y' = f_2(x, y)$ describe ray-mapping geometry. In the case discussed, it is fully defined by Eqs. (7). In order to switch from *ray-mapping-language* to *irradiance-transformation-language*, the following formula can be used:

$$I_\mathrm{out}(x', y')|J(x, y)| = I_\mathrm{in}(x, y) \tag{9}$$

where

$$J(x, y) = \begin{bmatrix} \dfrac{\partial f_1(x, y)}{\partial x} & \dfrac{\partial f_1(x, y)}{\partial y} \\ \dfrac{\partial f_2(x, y)}{\partial x} & \dfrac{\partial f_2(x, y)}{\partial y} \end{bmatrix} \tag{10}$$

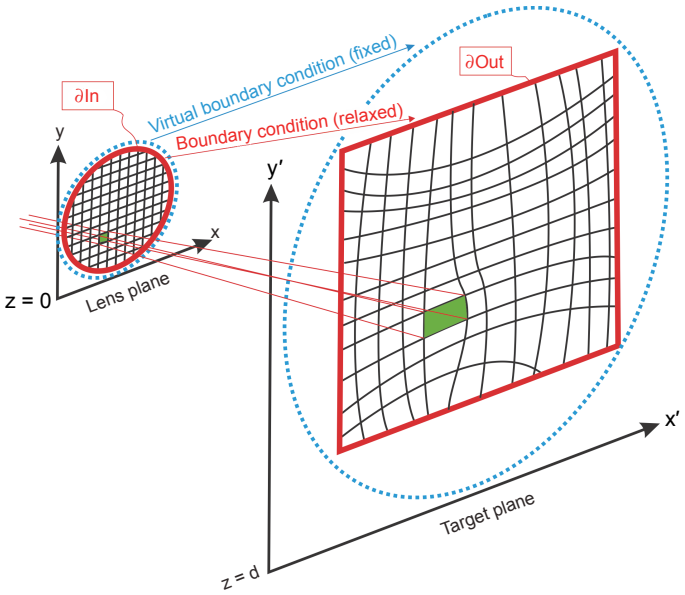

Fig. 3. Irradiance transformation considered as an expansion or contraction of infinitesimal quadrangles formed by four neighboring rays. Boundary condition is processed according to the relaxed scheme, as discussed in Section 3.1.

is a Jacobian matrix of ray mapping functions. It results from standard differential geometry principles of a surface continuous transformation (Fig. 3). Assuming lossless beam propagation, the relation between irradiance at any point $\mathbf{x}$ on the lens and corresponding point $\mathbf{x}' = \mathbf{f}(\mathbf{x})$ on the target is proportional to the expansion of the infinitesimal surface element ΔS surrounding point $\mathbf{x}$ and determined by four neighbouring rays. This expansion is in turn proportional to the determinant of Jacobian $|\partial \mathbf{f}/\partial \mathbf{x}|$.

By applying in the above equations, explicit forms of f_1, f_2 provided in Eqs. (7), one arrives at the following formula:

$$\det \nabla^2 z(x,y) = \frac{I_{\text{in}}(x,y)\dfrac{\sqrt{1+(z_x^2+z_y^2)(1-n_{\text{o}}^2)}}{K(z_x,z_y)^2}}{I_{\text{out}}(f_1(x,y),\ f_2(x,y))} \tag{11}$$

T a b l e. Equivalence of optimal mass transformation with quadratic cost function and irradiance transformation by freeform lens.

Optimal mass transportation	Freeform optics irradiance shaping
Scalar potential $\psi(\mathbf{x})$	Optical surface $z(x, y)$
Mass transfer plan $T(\mathbf{x})$	Ray-mapping $[f_1, f_2]$ (x, y)
Mass distributions:	Irradiance distributions:
– initial $f(\mathbf{x})$	– input (on the lens) $I_{\text{in}}(x, y)$
– final $g(\mathbf{x}')$	– output (on the target) $I_{\text{out}}(x', y')$

which is essentially a Monge–Ampère PDE. Comparing it with Eq. (2), one can recognize the analogies between optimal mass transportation problem and freeform optics beam shaping, which are summarized in the Table.

3. Numerical algorithm

Monge–Ampère PDE is a highly nonlinear, elliptic differential equation, generally not solvable in analytical sense. In order to implement the described model, a new numerical method has been proposed. Following the nine-point stencil discretization scheme [23]:

$$z_{xx}^{(i,j)} = \frac{1}{h^2}\left(z^{(i+1,j)} + z^{(i-1,j)} - 2z^{(i,j)}\right) \tag{12a}$$

$$z_{yy}^{(i,j)} = \frac{1}{h^2}\left(z^{(i,j+1)} + z^{(i,j-1)} - 2z^{(i,j)}\right) \tag{12b}$$

$$z_{xy}^{(i,j)} = \frac{1}{4h^2}\left(z^{(i+1,j+1)} + z^{(i-1,j-1)} - z^{(i-1,j+1)} - z^{(i+1,j-1)}\right) \tag{12c}$$

$$z_{x}^{(i,j)} = \frac{1}{2h}\left(z^{(i+1,j)} - z^{(i-1,j)}\right) \tag{12d}$$

$$z_{y}^{(i,j)} = \frac{1}{2h}\left(z^{(i,j+1)} - z^{(i,j-1)}\right) \tag{12e}$$

where $z^{(i,j)}$ corresponds to $z(x_i, y_j)$, as presented in Fig. 4, and applying the Gauss –Seidel approach, the computational algorithm has been built and implemented in MATLAB environment.

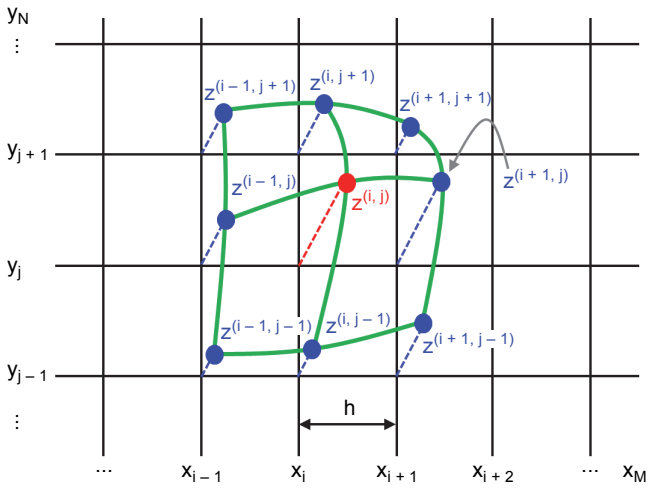

Fig. 4. Nine-point stencil scheme used to discretize the optical surface sag function and consider its derivatives as finite differences.

To construct the Gauss–Seidel iteration scheme, the analytical formula that expresses the value of the function at a general grid point $z^{(i,j)}$ by the values of the function in the neighbouring grid points, is required. Let's consider arithmetic averages of the discretized z function at the neighbouring grid points (Fig. 4), also in diagonal direction:

$$av_1^{(i,j)} = \left(z^{(i+1,j)} + z^{(i-1,j)}\right)/2 \tag{13a}$$

$$av_2^{(i,j)} = \left(z^{(i,j+1)} + z^{(i,j-1)}\right)/2 \tag{13b}$$

$$av_3^{(i,j)} = \left(z^{(i+1,j+1)} + z^{(i-1,j-1)}\right)/2 \tag{13c}$$

$$av_4^{(i,j)} = \left(z^{(i-1,j+1)} + z^{(i+1,j-1)}\right)/2 \tag{13d}$$

The second derivatives can be expressed by the application of the new dependent variables:

$$z_{xx}^{(i,j)} = \frac{2}{h^2}\left(av_1^{(i,j)} - z^{(i,j)}\right) \tag{14a}$$

$$z_{yy}^{(i,j)} = \frac{2}{h^2}\left(av_2^{(i,j)} - z^{(i,j)}\right) \tag{14b}$$

$$z_{xy}^{(i,j)} = \frac{1}{2h^2}\left(av_3^{(i,j)} - av_4^{(i,j)}\right) \tag{14c}$$

Substituting them into Equation (11) gives:

$$4\left(av_1^{(i,j)} - z^{(i,j)}\right)\left(av_2^{(i,j)} - z^{(i,j)}\right) - \frac{\left(av_3^{(i,j)} - av_4^{(i,j)}\right)^2}{4} = h^4 g^{(i,j)} \tag{15}$$

where $g^{(i,j)}$ represents the right side of the PDE:

$$g^{(i,j)} = \frac{I_{\text{in}}(x_i, y_i)}{I_{\text{out}}(f_1(x_i, y_i),\ f_2(x_i, y_i))} \frac{\sqrt{1 + (z_x^{(i,j)^2} + z_y^{(i,j)^2})(1 - n_{\text{o}}^2)}}{K(z_x^{(i,j)}, z_y^{(i,j)})^2} \tag{16}$$

In this way, the Monge–Ampère PDE (Eq. (11)) was transformed into a discrete quadratic formula – Eq. (16). Solving this equation, we obtain:

$$z^{(i,j)} = \frac{av_1^{(i,j)} + av_2^{(i,j)} - \sqrt{\left(av_1^{(i,j)} - av_2^{(i,j)}\right)^2 + \left(\frac{av_3^{(i,j)} - av_4^{(i,j)}}{2}\right)^2 + h^4 g^{(i,j)}}}{2} \tag{17}$$

The Gauss–Seidel method is iterative, which means that every grid point $z(i,j)$ is updated in a loop, based on eight neighbouring nodes $z(i \pm 1, j \pm 1)$. Concerning the initial iterate $z_{\text{init}}(i,j)$, a simple spherical surface was used. The only parameter – the surface curvature, was determined according to such a magnification of the incoming beam that on the target it completely overlaps the desired output distribution. Assuming that the input beam diameter is D_0, the distance to the target d and the maximum radial size D_{T}, the refractive surface radius of curvature R can be calculated from the standard *ynu* paraxial formulas, which gives:

$$R = \frac{D_0(n_0 - 1)d}{2D_{\text{T}}} \tag{18}$$

Spherical sag is given by the following general formula:

$$z(r) = \frac{r^2}{R_{\text{c}} + \sqrt{R_{\text{c}}^2 - r^2}} \tag{19}$$

By applying the Cartesian grid discretization and Eq. (18) in the above formula, the following initial iterate is obtained:

$$z_{\text{init}}^{(i,j)} = \frac{x_{i,j}^2 + y_{i,j}^2}{\dfrac{D_0(n_0 - 1)d}{2D_{\text{T}}} + \sqrt{\left(\dfrac{D_0(n_0 - 1)d}{2D_{\text{T}}}\right)^2 - (x_{i,j}^2 + y_{i,j}^2)}} \tag{20}$$

3.1. Relaxed boundary condition

It should be noted that in the discussed problem, a boundary condition is associated with the edge rays redistribution. Unfortunately, such boundary problem does not belong to typical Neumann or Dirichlet type, which are easy in implementation. Here, the rays corresponding to the outer rim of the beam ∂In should be directed to the edge of the target irradiance spatial distribution ∂Out. However, since both the input beam and target distribution can be generally of an arbitrary shape, also potentially composed of discontinuous factors, such boundary condition is non-trivial. It is not possible to predict *a priori*, which exactly output distribution edge point should intercept any specific input boundary ray. As such, any fixed predefined boundary-ray-mapping cannot be easily deduced. For this reason, the boundary condition in the presented approach is processed according to the relaxed scheme. Namely, around the real edge rays (rim of the input beam), additional single row envelope of abstract rays is supplied and computationally treated like a new boundary. In the first iteration, all the rays are directed according to the initial solution z_{init} geometry, which provides simple linear magnification $m = D_{\text{T}}/D_0$. As a result, no matter how complicated target irradiance geometry

is desired, the first iteration of the algorithm effectively sees the trivial boundary condition $\partial\text{Out} = m \cdot \partial\text{In}$. During the next iterations, abstract boundary rays remain in the positions obtained in the first iteration (they are not refreshed in the loop any more), however all other (real) rays positions evolve. Effectively, the rays neighbouring abstract frozen rays create real floating boundary. In other words, the boundary condition is adjusted by the bulk solution. It should be reminded that the proposed iterative method provides the result, which is associated with certain error (the quantitative example in the next paragraph). It means that the obtained output distribution shows certain level of discrepancy from the desired output distribution. The boundary rays will follow this error, which can be seen as a disadvantage of the discussed relaxed scheme. On the other side, the a.m. error can be minimized by the increased number of iterations and higher resolution (number of rays processed by the algorithm).

4. Case study

To verify its performance, the algorithm was tested against an extremely unconventional optical challenge – it was used to design such a freeform lens that would transform the input uniform collimated beam into three separate letters "WAT" – Polish abbreviation of Military University of Technology (Fig. 5).

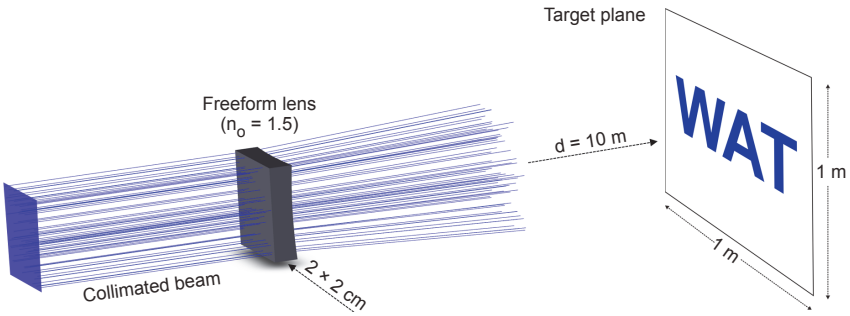

Fig. 5. Case study – designed freeform lens should transform the uniform input collimated beam into the shape of letters.

Lens surface and output distribution were discretized and processed as 300 × 300 discrete arrays ($i = 1, ..., 300; j = 1, ..., 300$). It took less than 4 minutes (CPU at 3.5 GHz, RAM 16 GB) to calculate the shape of the freeform surface $z^{(i,j)}$. The graphical representation of the obtained surface is presented in Fig. 6. It is smooth and convex, however showing no visual correspondence with the desired output distribution.

The array representation of freeform lens calculated in MATLAB was exported to ZEMAX in appropriately formatted *grid sag* file. The lens was tested both in a non-sequential and sequential mode, providing visually satisfactory performance in terms of the *obtained vs. desired* irradiance distribution (Fig. 7).

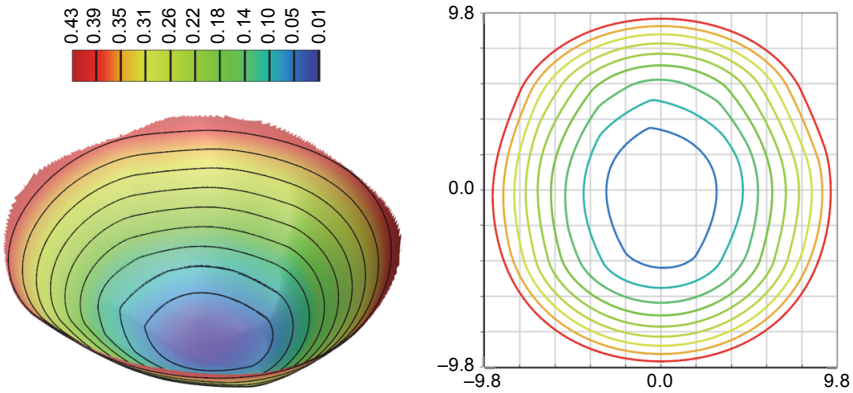

Fig. 6. The calculated freeform surface graphical representations.

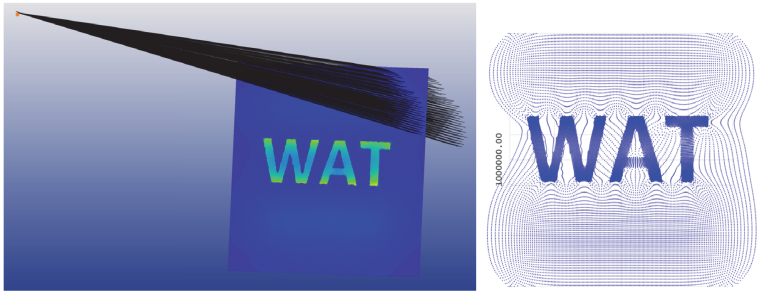

Fig. 7. Screenshots from ZEMAX implementation of the designed freeform lens (left – non-sequential mode and the obtained irradiance distribution, right – sequential mode standard spot diagram).

In order to quantitatively asses the lens performance, quality metrics based on fractional RMS measure [24] was applied

$$\mathrm{RMS} = \sqrt{\sum\left(\frac{I_{\mathrm{calc}} - I_{\mathrm{des}}}{I_{\mathrm{avg}}}\right)^2} \tag{21}$$

where I_{calc} is the calculated irradiance (obtained in ZEMAX), I_{des} is the desired (prescribed) irradiance and I_{avg} is an average irradiance applied for normalization reasons. Ideal irradiance shaping would result in RMS = 0. The obtained results generate RMS oscillating around 10% level (the screenshot presented in Fig. 7 corresponds to RMS = 10.9%). Such results can be improved even further, by increasing the number of iterations, however the incremental gain is smaller and smaller.

The algorithm is iterative and in the class of a challenging design type reported in this paper converged, so it was possible to run it as long as certain quality criterion is met. In the presented case, the loop was ordered to quit if the iteration-to-iteration surface averaged change was smaller than 50 nm. It should be noted however, that the

observed converging behaviour of the algorithm cannot be formally treated like a general convergence proof.

5. Conclusions

This paper deals with an astonishing link between mathematical theories governing two formally unconnected fields of engineering: sand (or generally – mass) optimal relocation in terrain *vs*. optical design of freeform lens. It is shown in details, how both issues lead to the same Monge–Ampère partial differential equation. Direct correspondence between mechanical quantities (mass density distributions, paths of transportation) on the one side and optical quantities (irradiances, freeform refractive surface shape) on the other side, is proved. Unfortunately, Monge–Ampère PDE is elliptic and highly nonlinear, so the solution in analytic sense is generally not achievable. In this work, the original numerical algorithm is proposed to solve this problem in order to design the refractive surface, capable of creating arbitrary light distribution. As an example, freeform lens which can transform the uniform collimated input beam into irradiance corresponding to "WAT" letters casted on the flat target located several meters away, is presented. Lens performance proved high efficiency in terms of the obtained irradiance distribution. The algorithm requires several minutes to obtain a satisfactory level of solution quality. Finally, optical surface is continuous and integrable, making it possible to be manufactured. The proposed method proved to be a valuable tool for freeform lens design, which is currently under worldwide consideration due to recently achieved manufacturability of such unconventional optical components.

References

[1] Monge G., *Mémoire sur la théorie des déblais et des remblais*, Histoire de l'Académie Royale des Sciences de Paris, 1781.

[2] Vershik A.M., *Long history of the Monge–Kantorovich Transportation Problem*, Sprienger, 2013.

[3] Rockafellar R.T., *Characterization of the subdifferentials of convex functions*, Pacific Journal of Mathematics 17(3), 1966, pp. 497–510.

[4] Glimm T., Oliker V., *Optical design of two-reflector systems, the Monge–Kantorovich mass transfer problem and Fermat's principle*, Indiana University Mathematics Journal 53(5), 2004, pp. 1255–1277.

[5] Rubinstein J., Wolansky G., *Intensity control with a free-form lens*, Journal of the Optical Society of America A 24(2), 2007, pp. 463–469.

[6] Oliker V., *Designing freeform lenses for intensity and phase control of coherent light with help from geometry and mass transport*, Archive for Rational Mechanics and Analysis 201(3), 2011, pp. 1013–1045.

[7] Ries H., Muschaweck J., *Tailored freeform optical surfaces*, Journal of the Optical Society of America A 19(3), 2002, pp. 590–595.

[8] Fournier F.R., Cassarly W.J., Rolland J.P., *Fast freeform reflector generation using source-target maps*, Optics Express 18(5), 2010, pp. 5295–5304.

[9] Michaelis D., Schreiber P., Bräuer A., *Cartesian oval representation of freeform optics in illumination systems*, Optics Letters 36(6), 2011, pp. 918–920.

[10] Bruneton A., Bäuerle A., Wester R., Stollenwerk J., Loosen P., *High resolution irradiance tailoring using multiple freeform surfaces*, Optics Express 21(9), 2013, pp. 10563–10571.

[11] BÖSEL C., GROSS H., *Ray mapping approach for the efficient design of continuous freeform surfaces*, Optics Express 24(13), 2016, pp. 14271–14282.
[12] ZEXIN FENG, LEI HUANG, GUOFAN JIN, MALI GONG, *Designing double freeform optical surfaces for controlling both irradiance and wavefront*, Optics Express 21(23), 2013, pp. 28693–28701.
[13] BÖSEL C., WORKU N. G., GROSS H., *Ray-mapping approach in double freeform surface design for collimated beam shaping beyond the paraxial approximation*, Applied Optics 56(13), 2017, pp. 3679–3688.
[14] RENGMAO WU, LIANG XU, PENG LIU, YAQIN ZHANG, ZHENRONG ZHENG, HAIFENG LI, XU LIU, *Freeform illumination design: a nonlinear boundary problem for the elliptic Monge–Ampére equation*, Optics Letters 38(2), 2013, pp. 229–231.
[15] RENGMAO WU, PENG LIU, YAQIN ZHANG, ZHENRONG ZHENG, HAIFENG LI, XU LIU, *A mathematical model of the single freeform surface design for collimated beam shaping*, Optics Express 21(18), 2013, pp. 20974–20989.
[16] PRINS C.R., TEN THIJE BOONKKAMP J.H.M., VAN ROOSMALEN J., JZERMAN W.L., TUKKER T.W., *A Monge –Ampère-solver for free-form reflector design*, SIAM Journal on Scientific Computing 36(3), 2014, pp. B640–B660.
[17] BRIX K., HAFIZOGULLARI Y., PLATEN A., *Designing illumination lenses and mirrors by the numerical solution of Monge–Ampère equations*, Journal of the Optical Society of America A 32(11), 2015, pp. 2227–2236.
[18] THOMPSON K.P., ROLLAND J.P., *Freeform optical surfaces: a revolution in imaging optical design*, Optics and Photonics News 23(6), 2012, pp. 30–35.
[19] FANG F.Z., ZHANG X.D., WECKENMANN A., ZHANG G.X., EVANS C., *Manufacturing and measurement of freeform optics*, CIRP Annals 62(2), 2013, pp. 823–846.
[20] GIMENEZ-BENITEZ P., MIÑANO J.C., BLEN J., ARROYO R.M., CHAVES J., DROSS O., HERNANDEZ M., FALICOFF W., *Simultaneous multiple surface optical design method in three dimensions*, Optical Engineering 43(7), 2004, pp. 1489–1502.
[21] CHAVES J., *Introduction to Nonimaging Optics*, 2nd Ed., CRC Press, 2016.
[22] DICKEY F.M., *Laser Beam Shaping: Theory and Techniques*, CRC Press, 2014.
[23] MAZUMDER S., *Numerical Methods for Partial Differential Equations*, Elsevier Academic Press, 2017.
[24] BORTZ J., SHATZ N., *Iterative generalized functional method of nonimaging optical design*, Proceedings of SPIE 6670, 2007, article ID 66700A.

Received September 7, 2017
in revised form December 8, 2017